

Lagrangian transport through surfaces in volume-preserving flows

Daniel Karrasch

ETH Zürich, Institute for Mechanical Systems,

*Leonhardstrasse 21, 8092 Zürich, Switzerland**

(Dated: January 2, 2022)

Abstract

Advective transport of scalar quantities through surfaces is of fundamental importance in many scientific applications. From the Eulerian perspective of the surface it can be quantified by the well-known integral of the flux density. The recent development of highly accurate semi-Lagrangian methods for solving scalar conservation laws and of Lagrangian approaches to coherent structures in turbulent (geophysical) fluid flows necessitate a new approach to transport from the (Lagrangian) material perspective. We present a Lagrangian framework for calculating transport of conserved quantities through a given surface in n -dimensional, fully aperiodic, volume-preserving flows. Our approach does not involve any dynamical assumptions on the surface or its boundary.

PACS numbers: 05.45.-a, 05.60.Cd, 47.10.-g, 47.11.-j, 47.52.+j

* kadanield@ethz.ch

I. INTRODUCTION

The transfer of a quantity along the motion of some carrying fluid, or *Lagrangian transport* for short, is of fundamental importance to a broad variety of scientific fields and applications. The latter include (geophysical) fluid dynamics [1–4], chemical kinetics [5], fluid engineering [6, 7] and plasma confinement [8]. Existing methods for computing transport have mostly been developed under certain assumptions on temporal behavior (steady or periodic time-dependence); spatial location (regions related to invariant manifolds such as lobe dynamics and dividing surfaces in transition state theory); state space dimension (2D); or restrict to a perturbation setting [9–13]. Recently, the problem of quantifying finite-time transport in aperiodic flows between distinct, arbitrary flow regions has been considered by Mosovsky *et al.* [14]. Mosovsky *et al.* [14] present a framework for describing and computing finite-time transport in n -dimensional (chaotic) volume-preserving flows, which relies on the reduced dynamics of an $(n-2)$ -dimensional “minimal set” of fundamental trajectories. In this paper, we present a Lagrangian approach to the complementary problem of transport through a fixed codimension-one surface over a finite-time interval in volume-preserving flows. This cannot be reformulated in the setting of [14], since (i) initial and final positions of surface-crossing particles are *a priori* unknown, and (ii) particles may cross the surface several times, possibly in opposite directions, leading to a net number of surface crossings different from one, in particular including zero.

The problem of computing the flux through a surface in general flows admits a well-known solution in terms of an integral of the flux density over the surface and the time interval of interest, cf. the left-hand side of Eq. (1). We view this approach as Eulerian, in that it involves instantaneous information (flux density) at fixed locations in space-time. However, recently two lines of research emerged that inevitably require a Lagrangian approach to the flux calculation.

The first is concerned with the numerical solution of advection equations (or, in the absence of sources, conservation laws) for conserved quantities by semi-Lagrangian methods, which enjoy geometric flexibility and the absence of Eulerian stability constraints [15, 16].

The second is concerned with transport by coherent vortices in oceanic flows, more precisely with the determination of the relevance of *coherent transport* [17–19], an open problem in physical oceanography and climate science. Coherent structures have long been studied in

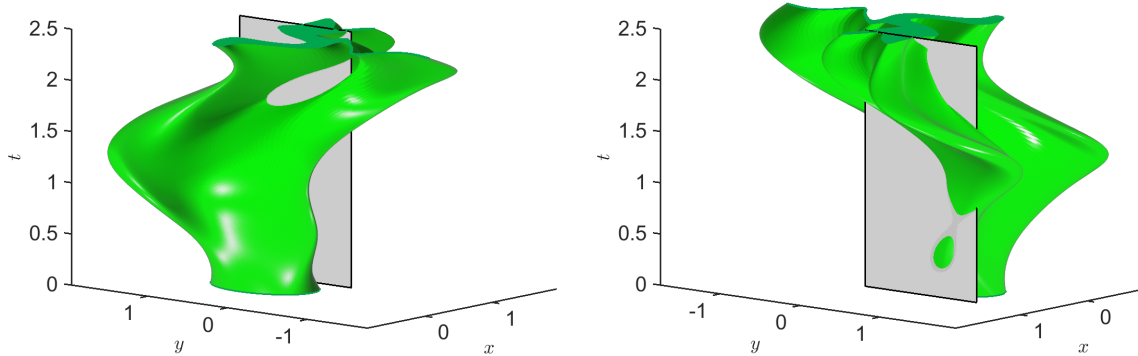


FIG. 1. Views from opposite directions on the evolution of an initial ellipse over time, and its intersection with a surface in extended state space. Computing the flux contribution by the material points originating from that ellipse in an Eulerian framework corresponds to computing the flux integral over the subset of the section which is contained in the interior of the cylindrical structure.

fluid dynamics [20], typically from an Eulerian point of view, i.e., by analyzing instantaneous snapshots of velocity fields. For transport-related issues, however, Lagrangian approaches have been shown to be better suited in that they are based on trajectory information [21–26].

Lagrangian methods identify certain material points as elements of a coherent structure. Determining a structure’s contribution to transport through a surface in an Eulerian manner requires knowledge about each point on the extended surface in space-time whether it is occupied by a material particle originating from a coherent structure. Additionally, the subset of points on the surface which are occupied by material particles of interest (such as a coherent structure) may be extremely complicated, cf. Fig. 1, especially in turbulent flows. As a consequence, an Eulerian integration of the flux density restricted to this subset is practically infeasible.

Conversely, from the material point of view, it is intuitive that the number of surface crossings of each individual Lagrangian particle is relevant to determine its flux contribution. First steps towards a classification of Lagrangian particles with respect to net number of curve crossings have been proposed for two-dimensional flows under additional technical assumptions by Zhang [27, 28]. In this paper, we solve the following more general *donating region problem* [16, Def. 1.2].

Problem 1 *For a given regular, divergence-free and time-dependent vector field $\mathbf{u}(t, \mathbf{x}) = \mathbf{u}_t(\mathbf{x})$, consider a conserved quantity $f(t, \mathbf{x}) = f_t(\mathbf{x})$, which satisfies the (scalar)*

conservation law in Eulerian form [29]

$$\partial_t f + \mathbf{u}_t \cdot \nabla f = 0.$$

Let \mathcal{C} be a compact, connected, embedded codimension-one surface \mathcal{C} in configuration space \mathbb{R}^n , and $\mathcal{T} = [0, \tau]$ be a compact time interval. The problem is to find pairwise disjoint sets $\mathcal{D}_k \subset \mathbb{R}^n$, indexed by $k \in \mathbb{Z}$, of Lagrangian particles at time $t = 0$, such that

$$\int_{\mathcal{C} \times \mathcal{T}} f \mathbf{u} \cdot \mathbf{n} = \sum_{k \in \mathbb{Z}} k \int_{\mathcal{D}_k} f_t|_{t=0}, \quad (1)$$

where \mathbf{n} is the unit normal vector field to \mathcal{C} characterizing the direction of positive flux.

While the left hand-side of (1) corresponds to the classical flux integral over the surface \mathcal{C} over time \mathcal{T} , i.e., an integral in Eulerian coordinates, the right-hand side is an integral solely over initial conditions, i.e., in Lagrangian coordinates. In Lagrangian terms, restriction to a given set of Lagrangian particles A of interest is then conveniently performed by intersection of \mathcal{D}_k 's with A , see also Fig. 4.

II. EULERIAN AND LAGRANGIAN COORDINATES

While Eulerian coordinates x are assigned to *spatial* points in a fixed frame of reference, Lagrangian coordinates p label *material* points and are usually taken as the Eulerian coordinates at some initial time, say, $t = 0$. The motion of material points is described by the flow φ , a mapping between initial positions p at time $t = 0$ and current positions x at time t , i.e., $\varphi_0^t(p) = x$. Thus, the flow map φ_0^t can be interpreted as a change from Lagrangian to Eulerian coordinates. The inverse flow map $\varphi_t^0 = (\varphi_0^t)^{-1}$ is hence the coordinate transformation from Eulerian to Lagrangian coordinates.

In fluid dynamics, there are two important characteristic curves associated with the flow [30], which we re-interpret in terms of Eulerian and Lagrangian coordinates.

A *path line through p* is the time-curve of a fixed Lagrangian particle p in Eulerian coordinates, i.e., $t \mapsto \varphi_0^t(p)$. In other words, the path line is a collection of Eulerian positions that the Lagrangian particle p will occupy at some time. Its time derivative, expressed in Eulerian coordinates, gives rise to the *velocity field*

$$\mathbf{u}_t(x) := \mathbf{u}(t, x) = \partial_t \varphi_0^t(\varphi_t^0(x)). \quad (2)$$

By construction, the path line through p is the solution of the initial value problem

$$\dot{x} = \mathbf{u}_t(x), \quad x(0) = p.$$

A *streak line through x* is the time-curve of a fixed Eulerian location x in Lagrangian coordinates, i.e., $t \mapsto \varphi_t^0(x)$. In other words, the streak line is a collection of material points that will occupy the Eulerian position x at some time. Its time derivative, expressed in Lagrangian coordinates, gives rise to the *streak vector field*

$$\mathbf{w}_t(p) := \mathbf{w}(t, p) = \partial_t \varphi_t^0(\varphi_0^t(p)).$$

By construction, the streak line through x is the solution of the initial value problem

$$\dot{p} = \mathbf{w}_t(p), \quad p(0) = x.$$

In this framework, the following algebraic relation between the velocity field \mathbf{u} and the streak vector field \mathbf{w} holds:

$$\mathbf{w}_t(p) = - \left(d\varphi_0^t(p) \right)^{-1} \mathbf{u} \left(t, \varphi_0^t(p) \right). \quad (3)$$

Equivalently, in global terms we have

$$\mathbf{w}_t = - \left(\varphi_t^0 \right)_* \mathbf{u}_t, \quad \mathbf{u}_t = - \left(\varphi_0^t \right)_* \mathbf{w}_t,$$

where the subindex $*$ denotes pushforward of vector fields by φ_t^0 and φ_0^t , resp.

Eq. (3) corrects the formula originally presented by Weinkauf and Theisel [31], and can be derived as follows. We need to find the velocity $\partial_t \varphi_t^0(x)$ along the streak line $t \mapsto \varphi_t^0(x)$ through x . Differentiation of the constant function $t \mapsto \varphi_0^t(\varphi_t^0(x)) = x$ with the shorthand notation $p = \varphi_t^0(x)$ yields

$$0 = \partial_t \varphi_0^t(p) + d\varphi_0^t(p) \partial_t \varphi_t^0(x).$$

Using (2) and the invertibility of the differential of the flow map with $d\varphi_0^t(p)^{-1} = d\varphi_t^0(x)$, we obtain Eq. (3) as claimed.

Finally, we recall that the flow φ is volume-preserving on \mathbb{R}^n if and only if the velocity field \mathbf{u} (or, equivalently, \mathbf{w}) is divergence-free [30].

III. TRANSPORT THROUGH SURFACES

In this section, we solve Problem 1 by analyzing the Eulerian-to-Lagrangian coordinate transformation from the differential topology viewpoint [32, 33].

A. Setting

We decompose the Eulerian-to-Lagrangian change of coordinates into two steps. First, we map Eulerian space-time points to their respective initial position at time $t = 0$, while keeping them on the same time slice, i.e.,

$$\Phi: \mathcal{T} \times \mathbb{R}^n \rightarrow \mathcal{T} \times \mathbb{R}^n, \quad (t, x) \mapsto (t, \varphi_t^0(x)) = (t, p).$$

The transformation Φ maps the (extended) section $\mathcal{H} = \mathcal{T} \times \mathcal{C}$, see Fig. 2, to the *streak surface* $\mathcal{S} := \Phi(\mathcal{H})$, see Fig. 3.

In extended Eulerian coordinates, trajectories (or, extended path lines) take the form $(t, \varphi_0^t(p))$; in extended Lagrangian coordinates, trajectories are simply vertical lines, i.e., $t \mapsto (t, p)$, see Fig. 3. Intersections of path lines with \mathcal{H} correspond one-to-one with intersections of \mathcal{S} with vertical lines.

In a second step, we project space-time points to their spatial coordinates by the canonical projection $\Pi: \mathcal{T} \times \mathbb{R}^n \rightarrow \mathbb{R}^n$ and introduce $\mathcal{D} := \Pi(\mathcal{S})$. We view the image of Π as the initial time slice of the extended state space and therefore parametrized by Lagrangian coordinates. By construction, we have for $\Psi := \Pi \circ \Phi$ the identity $\Psi(t, x) = \varphi_t^0(x)$, and it is exactly the particles from \mathcal{D} that cross \mathcal{C} within \mathcal{T} one way or another, possibly multiple times.

B. Counting net crossings – the degree

We study the differentiable map Ψ as a map between the two n -dimensional manifolds $\mathcal{H} \subset \mathcal{T} \times \mathbb{R}^n$ and $\mathcal{D} \subset \mathbb{R}^n$. To this end, we recall notions from differential topology and interpret them in our setting.

First, *regular points* $(t, x) \in \mathcal{H}$ are those for which the differential $d\Psi(t, x)$ is invertible. This is exactly the case, when the tangent space at \mathcal{S} does not contain the time component. Non-regular points (t, x) of Ψ are referred to as *critical points*, which correspond to $\mathbf{u}_t(x) \cdot \mathbf{n}(x) = 0$, i.e., $\mathbf{u}_t(x) = 0$ or $\mathbf{u}_t(x)$ being tangent to \mathcal{C} .

By Sard's theorem, the set of *critical values*, i.e., images of critical points, has measure zero in \mathcal{D} , even though the set of critical points may be large in \mathcal{H} . Consistently, critical points do not contribute to the Eulerian flux integral.

In the Eulerian setting, positive/negative crossings of a Lagrangian particle p through \mathcal{C} correspond to $\mathbf{u}_t(x) \cdot \mathbf{n}(x) \gtrless 0$ at corresponding intersections (t, x) . In the Lagrangian

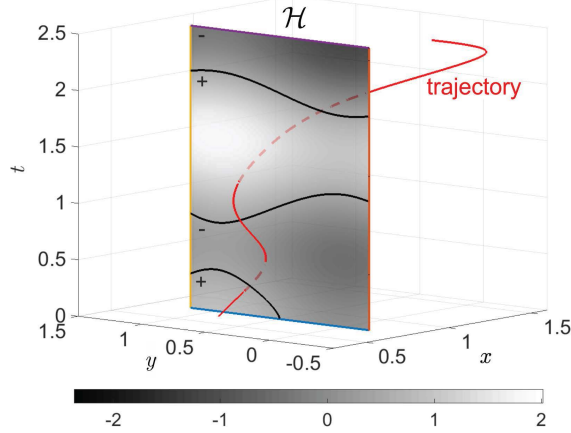


FIG. 2. Eulerian coordinates: Flux density on the section $\mathcal{H} = \mathcal{T} \times \mathcal{C}$, with $\mathcal{T} = [0, 2.5]$ and $\mathcal{C} = \{x = 0.75, -0.2 \leq y \leq 1.2\}$, bounded by blue, yellow, purple and brown lines. Zero-level curves of flux (black) and a sample trajectory (red, dashed when behind the section) launched at $(0.65, 0.85)$ are shown. Positive flux is directed in positive x -direction, flux direction through \mathcal{H} is indicated by $+/-$.

setting, positive/negative crossings are equivalent to crossings of the vertical line over p through \mathcal{S} from below/above w.r.t. the orientation on \mathcal{S} , see Fig. 3. This is formalized by $\det d\Psi \gtrless 0$, which geometrically means that $d\Psi(t, x)$ is orientation-preserving or orientation-reversing at the respective crossings of p . This in turn is well-defined for all crossings exactly for regular values p . Due to the compactness of \mathcal{H} the number of crossings of any regular value is finite.

The difference of positive and negative crossings, or, in other words, their net number, is hence given by the *degree of Ψ at $p \in \mathcal{D}$* ,

$$\deg(\Psi, p) := \sum_{(t, x) \in \Psi^{-1}(p) \cap \mathcal{H}} \text{sign}(\det(d\Psi(t, x))).$$

The degree function is locally constant, and can be used to define a partition of the set of Lagrangian particles, up to the measure zero set of critical values. Specifically, we define \mathcal{D}_k as the set of regular values p of Ψ such that $\deg(\Psi, p) = k$ for $k \in \mathbb{Z}$. Following [28], we refer to the \mathcal{D}_k 's as *donating regions of fluxing index k* . By construction, each \mathcal{D}_k contains the Lagrangian particles with only transversal crossings of which there are k net. In particular, all points that do not cross \mathcal{C} within \mathcal{T} are contained in \mathcal{D}_0 .

C. Area formula

Next, we restrict to the case $f \equiv 1$. We have the following identity for the degree of Ψ [34, Section 3.1.5, Thm. 6], which is a consequence of the *area formula* ([35] and [36, Thm. 5.3.7]):

$$\int_{\mathcal{H}} \det d\Psi(t, x) = \int_{\mathbb{R}^n} \deg(\Psi, p) dp = \sum_{k \in \mathbb{Z}} k \operatorname{vol}(\mathcal{D}_k).$$

The area formula is a generalization of the change of variables (in integral) formula to non-injective maps such as Ψ .

D. A useful identity

It remains to show that $\det d\Psi(t, x) = \mathbf{u}_t(x) \cdot \mathbf{n}(x)$. To this end, fix a regular point $(t, x) \in \mathcal{H}$. Then Ψ acts diffeomorphically between an open neighborhood \mathcal{U} of (t, x) in \mathcal{H} and its image $\mathcal{V} := \Psi(\mathcal{U})$ in \mathcal{D} . We may choose local coordinates on \mathcal{U} such that in (t, x) we have an orthonormal basis, i.e., $\mathbf{e}_t \in T_t \mathcal{T}$, $\operatorname{span}\{\mathbf{e}_2, \dots, \mathbf{e}_n\} = T_x \mathcal{C}$ and $\mathbf{e}_1 \in T_x^\perp \mathcal{H}$, with

$$dx(\mathbf{e}_1, \dots, \mathbf{e}_n) = 1 = dt \wedge dx(\mathbf{e}_t, \mathbf{e}_1, \dots, \mathbf{e}_n),$$

spanning unit volume. To avoid a discussion on delicate orientation issues, the following calculations involving determinants are to be read up to sign.

Next, we introduce a basis of $T_p \mathcal{D}$ by pushing forward the \mathbf{e}_i 's, i.e., $\mathbf{f}_i := (\varphi_t^0)_* \mathbf{e}_i$, which in turn span a unit space volume as well due to volume-preservation by φ :

$$\begin{aligned} dp(\mathbf{f}_1, \dots, \mathbf{f}_n) &= (\varphi_0^t)^* dx((\varphi_t^0)_* \mathbf{e}_1, \dots, (\varphi_t^0)_* \mathbf{e}_n) \\ &= dx(\mathbf{e}_1, \dots, \mathbf{e}_n) = 1. \end{aligned}$$

In the chosen coordinates, we get the following coordinate representation for \mathbf{u}_t

$$\mathbf{u}_t(x) = \sum_i u_t^i \mathbf{e}_i,$$

and $u_t^1 \neq 0$ by the regularity assumption on (t, x) . On the one hand, we have

$$\mathbf{u}_t \cdot \mathbf{n} = \det \begin{pmatrix} \mathbf{u}_t & \mathbf{e}_2 & \cdots & \mathbf{e}_n \end{pmatrix} = u_t^1.$$

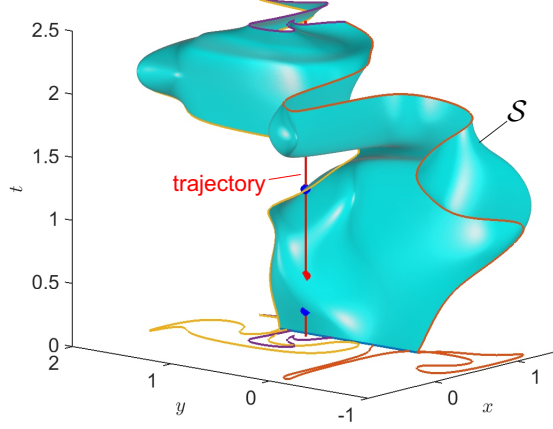


FIG. 3. Lagrangian coordinates: Streak surface \mathcal{S} and trajectory $(t, (0.65, 0.85))$ (red), which crosses \mathcal{S} twice in positive (blue balls) and once in negative (red ball) direction. The boundary curves correspond to the boundary curves in Fig. 2 with the respective colors. Their projections onto the $t = 0$ time slice are shown in the corresponding colors.

On the other hand, we first observe that

$$\det(d\varphi_0^t d\Psi) = \det d\varphi_0^t \det d\Psi = \det d\Psi, \quad (4)$$

since $\det d\varphi_0^t = 1$ for all t . Furthermore, it is readily seen that, in the chosen coordinates, $d\varphi_0^t d\Psi$ takes the form (recall $\partial_t \Psi = \mathbf{w}$)

$$d\varphi_0^t d\Psi = d\varphi_0^t \begin{pmatrix} | & 0 & \cdots & 0 \\ | & 1 & & \\ \mathbf{w} & & \ddots & \\ | & & & 1 \end{pmatrix} = \begin{pmatrix} \mathbf{u}_t & \mathbf{e}_2 & \cdots & \mathbf{e}_n \end{pmatrix},$$

where we have used Eq. (3). Due to (4), this proves $\det d\Psi(t, x) = u_t^1 = \mathbf{u}_t(x) \cdot \mathbf{n}(x)$ as required.

E. General conserved quantities

As noted in the Introduction, conserved quantities are constant along trajectories in volume-preserving flows. Therefore, we have $f_t(x) = f_0(\Psi(t, x))$, and the general area formula yields

$$\int_{\mathcal{H}} f_t(x) \det d\Psi(t, x) dt dx = \int_{\mathcal{H}} f_0(\Psi(t, x)) \det d\Psi(t, x) dt dx = \sum_k k \int_{\mathcal{D}_k} f_0(p) dp,$$

and together with $\det d\Psi(t, x) = \mathbf{u}_t(x) \cdot \mathbf{n}(x)$, Eq. (1) follows, and Problem 1 is solved.

F. The curvilinear case

Our result extends to the case when the state space is an n -dimensional, oriented smooth manifold \mathcal{M} with volume form ω . All differential topological notions and arguments work naturally in the manifold setting, and the useful identity between $d\Psi$ and the flux density was shown in local coordinates anyway. Note also that it does not require a (Riemannian) metric on \mathcal{M} . In the metric-free context, the Eulerian flux density is given by the interior product of \mathbf{u} and ω (or $\tilde{\omega}$), often denoted by $i_{\mathbf{u}_t}\omega$ or $\mathbf{u}_t \lrcorner \omega$.

G. The two-dimensional case

Our results for volume-preserving flows on \mathbb{R}^n simplify in the two-dimensional case considered by Zhang [27, 28] due to the well-known geometric characterization of the degree of Ψ at some regular value $p \in \mathcal{D} \subset \mathbb{R}^2$: it equals the *winding number* of p w.r.t. the closed curve $\Psi(\partial\mathcal{H})$ around p [37, Section 6.6]. The winding number counts the net number of turns of $\Psi(\partial\mathcal{H})$ around p under one counter-clockwise passage through $\partial\mathcal{H}$, see Fig. 4.

In the 2D case, we find the donating regions \mathcal{D}_k of fluxing index k as follows. The boundary $\partial\mathcal{H}$ of the extended section \mathcal{H} is a closed curve, just as its image under Ψ . In Fig. 4 its image corresponds to the concatenation of the section (blue), one streakline (say, yellow), the backward image of the section (purple) and the other streakline (brown). This closed curve gives rise to possibly several connected components through its self-intersections, and the winding number is constant on each such component. In the case of constant density, the Lagrangian flux calculation reduces to the computation of the enclosed area of each component, multiplied by its winding number and summed up.

In summary, we have generalized the main result of [28], in which only the issue of counting net crossings was treated under additional assumptions from a different methodological perspective. Note also that for the isolated counting aspect, our characterization in terms of $\deg(\Psi)$, or winding number in 2D, is also valid in the case of a compressible velocity field \mathbf{u} .

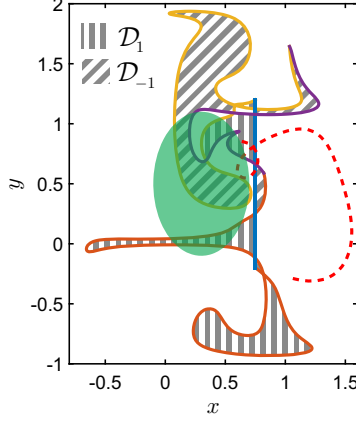


FIG. 4. Donating regions divided in cells with winding number/fluxing index $+1$ (vertically hatched), -1 (diagonally hatched) and 0 (white). The section \mathcal{C} (blue), the streak lines through the boundary points of \mathcal{C} (yellow & brown), and the backward image of the section (purple) correspond to the curves shown on the bottom layer in Fig. 3. The dashed curve (red) is the path line corresponding to the trajectory in Figs. 2 and 3. The ellipse (dark green) corresponds to the set of Lagrangian particles whose flow evolution is shown in Fig. 1.

IV. ILLUSTRATING EXAMPLE

For the readers' convenience, we consider only a simple illustrating example with parameters chosen such that figures may be generated which are both appealing and comprehensible and which support visually the abstract theory derived in Section III.

For the fluid motion, consider an array of vortices, given by the Hamiltonian

$$H(x, y) = A \sin(\pi x) \sin(\pi y),$$

subject to an aperiodic, spatially uniform spiraling forcing given by $F(t) = \begin{pmatrix} t \sin(\pi t) & t \cos(\pi t) \end{pmatrix}^\top$. The velocity field is hence

$$\mathbf{u}(t, x, y) = \begin{pmatrix} \partial_y H(x, y) - t \sin(\pi t) \\ -\partial_x H(x, y) - t \cos(\pi t) \end{pmatrix}.$$

We set the material density $f \equiv 1$, the section to $\mathcal{C} = \{x = 0.75, -0.2 \leq y \leq 1.2\}$, and the time interval to $\mathcal{T} = [0, 2.5]$. We show the Eulerian flux density on the surface $\mathcal{H} = \mathcal{C} \times \mathcal{T}$ in Fig. 2, in which \mathcal{H} is bounded by blue, yellow, purple and brown lines. Also shown are zero-level curves (black) of the flux density to distinguish between regions of positive (+)

and negative (-) flux. For reference, we show a trajectory in Eulerian coordinates with 3 intersections, two with positive and one with negative orientation.

In Fig. 3, we show the same objects, yet in Lagrangian coordinates, with boundary curves and reference trajectory in the same coloring as in Fig. 2. Also shown are projections of the boundary curves to the initial time slice. Fig. 4 shows the projected boundary curves, i.e., $\Psi(\partial\mathcal{H})$, viewed from above, with enclosed connected components hatched according to their winding number.

For a numerical validation of Eq. (1), we compute its left-hand side, i.e., the Eulerian integral, by numerical quadrature, which yields a transport value of -0.142 ; and the right-hand side, i.e., the Lagrangian integral, yields a transport value of -0.141 , with relative error below 1%; see [15] for improvements of area calculations via spline-approximation of polygon boundaries. Note that, in practice, the numerical integration of the Eulerian integral becomes more challenging in case the surface \mathcal{H} is curved and requires a parametrization. In contrast, this does not add any difficulty in the Lagrangian framework.

As mentioned in the Introduction, the real strength of the Lagrangian transport approach is when the interest is in the flux contribution by given set of material points, say, A , such as the ellipse in Figs. 1 and 4 (dark green). In the present case, this computation reduces to $\text{vol}(A \cap \mathcal{D}_1) - \text{vol}(A \cap \mathcal{D}_{-1})$, which gives a transport contribution of -0.1061 .

At first sight, this seems to be paradox, since the entire ellipse is launched from one side of the section, and Fig. 1 indicates that at the end of the time interval, parts of the material ended on the other side of the section. Going from the first to the latter side corresponds to positive flux, and one is led to think there should be an overall positive transport contribution. A closer inspection of Fig. 1, however, reveals that most of the material which is advected to the other side has actually not crossed the section, but has flown around it. Moreover, much of the material which has flown around has actually crossed the section in negative direction, thus yielding an overall negative flux contribution of the ellipse.

ACKNOWLEDGMENTS

I would like to thank Simon Eugster, Florian Huhn and Dietmar Salamon for useful discussions, as well as George Haller for helpful comments on an earlier version of the

manuscript. David Legland’s `geom2d`-library for MATLAB was of great help in the generation of Fig. 4.

-
- [1] J. M. Ottino, *The Kinematics of Mixing: Stretching, Chaos, and Transport* (Cambridge University Press, 1989).
 - [2] S. Wiggins, *Chaotic Transport in Dynamical Systems*, Interdisciplinary Applied Mathematics, Vol. 2 (Springer, 1992).
 - [3] R. M. Samelson and S. Wiggins, *Lagrangian Transport in Geophysical Jets and Waves*, Interdisciplinary Applied Mathematics, Vol. 31 (Springer, 2006).
 - [4] J. Lin, D. Brunner, C. Gerbig, A. Stohl, A. Luhar, and P. Webley, eds., *Lagrangian Modeling of the Atmosphere*, Geophysical Monograph Series, Vol. 200 (American Geophysical Union, 2013).
 - [5] W. M. Deen, *Analysis of transport phenomena*, 2nd ed. (Oxford University Press, 2013).
 - [6] Z. Pouransari, M. F. M. Speetjens, and H. J. H. Clercx, “Formation of coherent structures by fluid inertia in three-dimensional laminar flows,” *J. Fluid Mech.* **654**, 5–34 (2010).
 - [7] M. F. M. Speetjens, E. A. Demissie, G. Metcalfe, and H. J. H. Clercx, “Lagrangian transport characteristics of a class of three-dimensional inline-mixing flows with fluid inertia,” *Phys. Fluids* **26**, 113601 (2014).
 - [8] A. H. Boozer, “Physics of magnetically confined plasmas,” *Rev. Mod. Phys.* **76**, 1071–1141 (2005).
 - [9] R. S. MacKay, J. D. Meiss, and I. C. Percival, “Transport in Hamiltonian systems,” *Physica D* **13**, 55–81 (1984).
 - [10] R. S. MacKay, “Flux over a saddle,” *Phys. Lett. A* **145**, 425 – 427 (1990).
 - [11] R. S. MacKay, “Transport in 3D volume-preserving flows,” *J. Nonlinear Sci.* **4**, 329–354 (1994).
 - [12] V. Rom-Kedar and S. Wiggins, “Transport in two-dimensional maps,” *Arch. Ration. Mech. Anal.* **109**, 239–298 (1990).
 - [13] S. Balasuriya, “Cross-separatrix flux in time-aperiodic and time-impulsive flows,” *Nonlinearity* **19**, 2775 (2006).
 - [14] B. A. Mosovsky, M. F. M. Speetjens, and J. D. Meiss, “Finite-Time Transport in Volume-Preserving Flows,” *Phys. Rev. Lett.* **110**, 214101 (2013).

- [15] Q. Zhang, “Highly accurate Lagrangian flux calculation via algebraic quadratures on spline-approximated donating regions,” *Comput. Methods Appl. Mech. Engrg.* **264**, 191–204 (2013).
- [16] Q. Zhang, “On a Family of Unsplit Advection Algorithms for Volume-of-Fluid Methods,” *SIAM J. Numer. Anal.* **51**, 2822–2850 (2013).
- [17] C. Dong, J. C. McWilliams, Y. Liu, and D. Chen, “Global heat and salt transports by eddy movement,” *Nature Communications* **5**, 1–6 (2014).
- [18] Z. Zhang, W. Wang, and B. Qiu, “Oceanic mass transport by mesoscale eddies,” *Science* **345**, 322–324 (2014).
- [19] F. Huhn, M. Mazloff, T. Schneider, and G. Haller, “Coherent Lagrangian eddies and coherent transport in the Agulhas leakage,” (2015), in preparation.
- [20] A. K. M. Fazle Hussain, “Coherent structures and turbulence,” *J. Fluid Mech.* **173**, 303–356 (1986).
- [21] G. Haller, “Lagrangian Coherent Structures,” *Annu. Rev. Fluid Mech.* **47**, 137–161 (2015).
- [22] G. Haller and F. J. Beron-Vera, “Coherent Lagrangian vortices: the black holes of turbulence,” *J. Fluid Mech.* **731**, R4 (2013).
- [23] D. Karrasch, F. Huhn, and G. Haller, “Automated detection of coherent Lagrangian vortices in two-dimensional unsteady flows,” *Proc. R. Soc. A* **471**, 20140639 (2015).
- [24] G. Froyland and K. Padberg-Gehle, “Almost-Invariant and Finite-Time Coherent Sets: Directionality, Duration, and Diffusion,” in *Ergodic Theory, Open Dynamics, and Coherent Structures*, Springer Proceedings in Mathematics & Statistics, Vol. 70, edited by W. Bahsoun, C. Bose, and G. Froyland (Springer, 2014) pp. 171–216.
- [25] T. Ma and E. M. Boltt, “Differential Geometry Perspective of Shape Coherence and Curvature Evolution by Finite-Time Non-hyperbolic Splitting,” *SIAM J. Appl. Dyn. Syst.* **13**, 1106–1136 (2014).
- [26] R. Mundel, E. Fredj, H. Gildor, and V. Rom-Kedar, “New Lagrangian diagnostic for characterizing fluid flow mixing,” *Phys. Fluids* **26**, 126602 (2014).
- [27] Q. Zhang, “On Donating Regions: Lagrangian Flux through a Fixed Curve,” *SIAM Review* **55**, 443–461 (2013).
- [28] Q. Zhang, “On generalized donating regions: Classifying Lagrangian fluxing particles through a fixed curve in the plane,” *J. Math. Anal. Appl.* **424**, 861–877 (2015).
- [29] The Lagrangian form is $\frac{Df}{Dt} = 0$ with $\frac{D}{Dt}$ the material derivative. Physically, this means that

- the scalar f does not change along particle motions.
- [30] G. K. Batchelor, *An Introduction to Fluid Dynamics*, Cambridge Mathematical Library (Cambridge University Press, 2000).
 - [31] T. Weinkauff and H. Theisel, “Streak Lines as Tangent Curves of a Derived Vector Field,” *Visualization and Computer Graphics*, IEEE Transactions on **16**, 1225–1234 (2010).
 - [32] J. W. Milnor, *Topology from the Differentiable Viewpoint* (The University Press of Virginia, 1965).
 - [33] M. W. Hirsch, *Differential Topology* (Springer, 1976).
 - [34] M. Giaquinta, G. Modica, and J. Souček, *Cartesian Currents in the Calculus of Variations I: Cartesian Currents*, *Ergebnisse der Mathematik und ihrer Grenzgebiete*, Vol. 37 (Springer, 1998).
 - [35] H. Federer, *Geometric Measure Theory*, *Classics in Mathematics* (Springer, 1996).
 - [36] S. G. Krantz and H. Parks, *Geometric Integration Theory*, *Cornerstones* (Birkhäuser, 2008).
 - [37] K. Deimling, *Nonlinear Functional Analysis* (Springer, 1985).